Published in final edited form as:
Hepatology. 2010 November ; 52(5): 1819–1828. doi:10.1002/hep.23883.

ATP release and P2 receptor-mediated secretion in small and large mouse cholangiocytes

Kangmee Woo[1], **Meghana Sathe**[1], **Charles Kresge**[1], **Victoria Esser**[2], **Yoshiyuki Ueno**[5], **Julie Venter**[3], **Shannon S. Glaser**[3], **Gianfranco Alpini**[3,4], and **Andrew P. Feranchak**[1]

[1]Department of Pediatrics, University of Texas Southwestern Medical Center, Dallas, TX 75390-9063

[2]Internal Medicine, University of Texas Southwestern Medical Center, Dallas, TX 75390-9063

[3]Research, Central Texas Veterans Health Care System, Scott & White Digestive Disease Research Center, Scott & White, Texas A&M Health Science Center College of Medicine, Temple, TX

[4]Department of Medicine, Division Gastroenterology, Texas A&M Health Science Center College of Medicine, Temple, TX

[5]Tohoku University, School of Medicine, Sendai, Japan

Abstract

Adenosine triphosphate (ATP) is released from cholangiocytes into bile and is a potent secretogogue by increasing intracellular Ca^{2+} and stimulating fluid and electrolyte secretion via binding purinergic (P2) receptors on the apical membrane. While morphological differences exist between small and large cholangiocytes (lining small and large bile ducts, respectively), the role of P2 signaling has not been previously evaluated along the intrahepatic biliary epithelium. The aim of these studies therefore was to characterize ATP release and P2-signaling pathways in small (MSC) and large (MLC) mouse cholangiocytes. The findings reveal that both MSC and MLC express P2 receptors, including P2X4 and P2Y2. Exposure to extracellular nucleotides (ATP, UTP, or Bz-ATP) caused a rapid increase in $[Ca^{2+}]_i$ and in transepithelial secretion (I_{sc}) in both cell types, which was inhibited by the Cl^- channel blockers NPPB or niflumic acid. In response to mechanical stimulation (flow/shear or cell swelling secondary to hypotonic exposure) both MSC and MLC exhibited a significant increase in the rate of exocytosis which was paralleled by an increase in ATP release. Mechanosensitive ATP release was 2-fold greater in MSC compared to MLC. ATP release was significantly inhibited by disruption of vesicular trafficking by monensin in both cell types. *Conclusion*: These findings suggest the existence of a P2-signaling axis along intrahepatic biliary ducts with the “upstream” MSC releasing ATP, which can serve as a paracrine signaling molecule to “downstream” MLC stimulating Ca^{2+}-dependent secretion. Additionally, in MSC, which do not express the Cystic Fibrosis Transmembrane Conductance Regulator (CFTR), Ca^{2+}-activated Cl^- efflux in response to extracellular nucleotides represents the first secretory pathway clearly identified in these cholangiocytes derived from the small intrahepatic ducts.

Contact Information: Andrew Feranchak, M.D., UT Southwestern Medical Center, 5323 Harry Hines Boulevard, Dallas, TX 75390-9063, Telephone: 214-648-3118, FAX: 214-648-2673, drew.feranchak@UTSouthwestern.edu.

Disclosures: None.

Author contributions: K.W. and A.P.F. designed research; Y.U., J.V., S.G., and G.A. isolated and developed cell models; K.W., M.S., C.K., V.E., S.G., and A.P.F., performed research; K.W., M.S., and A.P.F. analyzed data; K.W. and A.P.F. wrote the paper.

Background and Aims

Cholangiocytes, the epithelial cells that form the intrahepatic bile ducts, represent an important component of the bile secretory unit. While bile formation is initiated at the hepatocyte canalicular membrane, cholangiocytes subsequently modify the composition of bile through regulated ion secretion throughout the network of bile ducts (1). Interestingly, secretory mechanisms along the intrahepatic bile ducts are not uniform. In all biliary models studied, including human, rat, and mouse bile ducts, cholangiocytes are known to be morphologically and functionally heterogeneous. Large cholangiocytes, from large ducts, express secretin receptors on the basolateral membrane and CFTR and the HCO_3^-/Cl^- anion exchanger 2 (AE2) on the apical membrane (2–4), and hence respond to secretin with an increase in intracellular [cAMP], and subsequent Cl^- and HCO_3^- efflux into the lumen. Conversely, small cholangiocytes, from small ducts, do not express secretin receptors, CFTR, or HCO_3^-/Cl^- exchanger and do not exhibit a secretory response to secretin (3). In human liver, parallel to the findings observed in the rat and mouse, secretin-stimulated duct secretory activity is heterogeneous, since only medium and large interlobular bile ducts express the Cl^-/HCO_3^- exchanger AE2 (5).

Recently, secretion mediated by extracellular nucleotides (e.g. ATP) acting on purinergic (P2) receptors on the luminal membrane of biliary epithelial cells has emerged as functionally important. ATP is present in bile (6), and binding of ATP to P2 receptors increases K^+ (7,8) and Cl^- efflux from isolated cholangiocytes (9,10) and dramatically increases transepithelial secretion in biliary epithelial monolayers (10,11). Indeed, the magnitude of the secretory response to ATP is 2- to 3-fold greater than that to cAMP (10). Interestingly, recent evidence suggests that even cAMP-stimulated bile flow is mediated by ATP release into the duct lumen and stimulation of apical P2 receptors (12). Together, these studies challenge and extend the conventional model that centers on the concept that cAMP-dependent opening of CFTR-related Cl^- channels is the driving force for cholangiocyte secretion. Rather the operative regulatory pathways appear to take place within the lumen of intrahepatic ducts, where release of ATP into bile is a final common pathway controlling ductular bile formation. In light of recent studies demonstrating that the mechanical effects of fluid-flow or shear stress at the apical membrane of biliary epithelial cells is a robust stimulus for ATP release (13), a model emerges in which mechanosensitive ATP release and Cl^- secretion is a dominant pathway regulating biliary secretion.

While cholangiocytes express a repertoire of both P2X and P2Y receptors (11,14,15), it is unknown if expression differs between small and large cholangiocytes and/or if functional differences exist in ATP release and signaling along the bile duct. The aim of the current studies therefore was to determine if a potential P2-signaling axis may exist along the bile duct by evaluating mechanosensitive ATP release and exocytosis, P2 receptor expression and function, and secretion mediated by extracellular nucleotides in both small and large mouse cholangiocytes.

Materials and Methods

Cell models

Studies were performed in mouse cholangiocytes isolated from normal mice (BALB/c) and immortalized by transfection with the SV40 large-T antigen gene (4). These cells demonstrate identical properties to freshly isolated small and large mouse cholangiocytes (3). Cells were maintained in culture as described (3,4). Additional studies of P2 receptor expression were performed in primary cholangiocytes isolated from C57BL/6 mice (Charles River, Wilmington, MA) as previously described (16,17). All animal experiments were performed in accordance with a protocol approved by the Scott and White Institutional

Animal Care and Use Committee and in accordance with the Guide for the Care and Use of Laboratory Animals published by the US National Institutes of Health (NIH Publication No. 85-23, revised 1996).

Total RNA isolation and RT-PCR analysis

Total RNA was extracted using TRIZOL Reagent (Invitrogen, Carlsbad, CA) and 1 μg of RNA was reverse transcribed in the presence of 100 pmol of oligo-dT primer. Aliquots of 5% of the total cDNA were amplified with TaqDNA Polymerase in a reaction mixture containing 20 pmol of 5' and 3' primers specifically designed for various P2X and P2Y receptors (supplemental Methods and Table S1).

Measurement of $[Ca^{2+}]_i$

MLC and MSC were grown to confluence on cover-glass (Figure 2), loaded with 2.5 μg/ml of fura-2 AM (TEF Laboratories, Austin TX), placed in a perfusion chamber (RC-25F/PHA, Warner Instruments) on the stage of an inverted fluorescence microscope (Nikon TE2000), and the inflow and outflow ports were connected to a syringe pump. Changes of $[Ca^{2+}]_i$ were measured at excitation wavelength of 340 nm (calcium-bound fura-2) and 380 nm (calcium-free fura-2), and emission wavelength of 510 nm and $[Ca^{2+}]_i$ was calculated.

Immunostaining

Confluent MSC and MLC were incubated with acetylated α-tubulin antibody (Sigma), as a marker for the primary cilium, and rhodamine phalloidin (Invitrogen) to label actin. Imaging was performed using a Perkin Elmer UltraVIEW ERS spinning disk confocal microscope (Perkin Elmer, Boston, MA). Imaris 5.0 (Bitplane Inc., Saint Paul, MN) was used for 3-dimensional volume rendering of z-stacks.

Measurement of exocytosis

Exocytosis was assessed by real time imaging using the fluorescent dye FM1-43 (Molecular Probes, Inc., Eugene, OR) as previously described (18). FM1-43 is weakly fluorescent in aqueous solution, but its fluorescence increases > 300-fold when it binds plasma membrane and, therefore, it is a useful dye for the measurement of increased plasma membrane due to fusion of vesicle membrane with the plasma membrane during exocytosis.

Measurement of ATP release

Bulk ATP release was studied from confluent cells using the luciferin-luciferase (L-L) assay as previously described (13,19,20). Cell swelling was induced by adding water to dilute media 33% and defined shear stress was applied to confluent cells in a parallel plate chamber. All luminescence values are reported as relative change from basal luminescence per total protein level in the sample (μg/ml) to control for any potential differences in luciferase activity or confluency between samples, respectively. Detailed protocols for measurements of ATP release, ATP degradation, protein levels and LDH are described in supplemental Methods.

Transepithelial Cl^- secretion

MLC and MSC were grown on collagen-coated polycarbonate filters with a pore size of 0.4 μm (Costar, Cambridge, MA) and the transmembrane resistance was measured daily (EVOHM, world Precision Instruments, Sarasota, FL) (21). Filters were mounted in an Ussing chamber, filled with standard buffer solution, and transepithelial short-circuit current response (I_{sc}) was measured under 0 mV voltage-clamp conditions through agar bridges connected to Ag-AgCl electrodes using an epithelial voltage clamp amplifier (model EC-825; Warner Instruments, MRA International, Naples, FL). The I_{sc} represents the net

sum of the transepithelial fluxes of anion and cation and the level of ion secretion (11). Studies included paired, same-day monolayers to minimize any potential effects of day-to-day variability.

Reagents and Statistics

Detailed descriptions of the reagents, buffer solutions, experimental protocols, and statistical analysis are provided in Supplemental Materials.

Results

Large and small cholangiocytes express a repertoire of P2X and P2Y receptors

In both MLC and MSC cDNAs were probed with oligonucleotide primers specific to the seven P2X subtypes and seven P2Y subtypes in mouse (shown in supplemental Table S1) and amplified using RT-PCR method. Representative studies are shown in MLC and MSC (Figure 1), and in primary isolated cholangiocytes (Supplemental Figure 1). In both MLC and MSC, clear bands corresponding to P2X4 and all seven P2Y receptors (1,2,4,6,11,12 and 13) are present. These results are consistent with previous studies of human and rat biliary cells where a predominance of P2X4 and multiple P2Y receptors were observed (11, 14, 15).

Agonist profile of nucleotide-stimulated Ca^{2+} fluorescence

To establish the functional significance of mouse cholangiocyte P2 receptor expression, MSC and MLC were grown to confluence (Figure 2) and changes in Ca^{2+} fluorescence measured in response to P2Y and P2X agonists. Exposure to ATP, UTP, a P2Y-preferring agonist, or Bz-ATP, a P2X-preferring agonist, all resulted in significant increases in $[Ca^{2+}]_i$ in both MLC and MSC (Figure 3). The ATP-stimulated increase in $[Ca^{2+}]_i$ was abolished by the P2Y receptor blocker, suramin (Figure 3D). Together, these results demonstrate that P2X4 and P2Y receptors expressed by both MLC and MSC are functionally active. No differences were observed between MLC and MSC in either the magnitude or kinetics of the Ca^{2+} response to any of the nucleotides.

Functional role for P2 receptors in transepithelial secretion

When cultured as described, both MSC and MLC developed an increase in transmembrane resistance by day 3 signifying the development of confluent monolayers with tight junctions (Figure 4A). When mounted in an Ussing chamber, confluent MLC and MSC monolayers exhibited a basal I_{sc}, reflecting transepithelial secretion, which increased dramatically in response to the addition of ATP (100 μM) to the apical chamber (Figure 4B and 4C). The nucleotide-stimulated I_{sc} was significantly inhibited by the non-specific Cl^- channel blocker, NPPB, or by the Ca^{2+}-activated Cl^- channel blocker niflumic acid (Figure 4C and 4F). Additionally, pre-incubation with the IP3 receptor blocker, 2-APB, significantly inhibited the ATP-stimulated increase in I_{sc} in both MLC and MSC (Fig.4C). In separate experiments, the effect of apical versus basolateral P2 receptor stimulation on the I_{sc} was determined. For both MSC and MLC, an increase in the I_{sc} was observed when nucleotides were added to either chamber, consistent with functional expression of P2 receptors on both apical and basolateral membranes. The magnitude of the change in I_{sc} was similar when nucleotides were added to either apical or basolateral compartments for all nucleotides tested except for UTP which caused a significantly greater increase in I_{sc} when added apically versus basolateral addition. Thus, both MSC and MLC express functional P2 receptors on both apical and basolateral membranes. Nucleotide binding to P2 receptors causes an increase in $[Ca^{2+}]_i$, predominantly through an IP3 receptor-dependent mechanism, which stimulates Ca^{2+}-activated Cl^- channels, and results in transepithelial secretion. To our

knowledge, these represent the first integrated I_{sc} measurements of transepithelial secretion in mouse cholangiocytes. Furthermore, in MSC, which do not express CFTR, Ca^{2+}-activated Cl^- efflux in response to extracellular nucleotides represents the first secretory pathway clearly identified in these cells derived from the small intrahepatic ducts.

Mechanosensitive ATP release

In human biliary cells and normal rat cholangiocyte monolayers, mechanical stimulation (22), shear stress (13), and cell swelling secondary to hypotonic exposure (22), have all been identified as significant stimuli for ATP release. Studies were performed to determine if these mechanical stimuli result in a similar increase in the magnitude of ATP release in mouse cholangiocytes. First, in response to hypotonic exposure (33% dilution) to stimulate cell swelling, a rapid and large increase in ATP release was observed in both MLC and MSC (Figure 5A). The magnitude of the response, which peaked within 30 seconds, was significantly greater in MSC versus MLC (Figure 5A and 5C). Separate studies were performed to assess the effects of shear on ATP release. Under low shear conditions (shear 0.08 dyne/cm^2) no increase in ATP release was observed; however, increasing shear to 0.64 dyne/cm^2 caused a rapid relative increase in ATP release in both MLC and MSC, and again the magnitude of the peak response was significantly greater in MSC versus MLC ($p<0.05$, Figure 5B and 5C). No difference was noted in LDH measurements pre- or post-stimulus, for either hypotonic or shear exposure, excluding cell lysis as contributing to measured ATP (data not shown). In other biliary models, ATP release has been linked to exocytosis (18). To determine if exocytosis contributes to ATP release in MLC and MSC, studies were performed in the presence or absence of monensin, a carboxylic ionophore known to dissipate the transmembrane pH gradients in Golgi and lysosomal compartments and disrupt vesicular trafficking. In both MLC and MSC, monensin significantly inhibited swelling-induced (33% hypotonic exposure) ATP release (Figure 5D). Thus, both MSC and MLC exhibit mechanosensitive ATP release which is dependent on intact vesicular trafficking pathways. Additionally, the magnitude of mechanosensitive ATP release is significantly greater (~2-fold) in MSC compared to MLC.

Mechanosensitive exocytosis

To determine if the difference in ATP release observed between MSC and MLC are the result of generalized differences in total cellular exocytosis, rates of exocytosis were measured in response to mechanical stimuli in both cell types. After equilibration with FM1-43, cells were exposed to hypotonic buffer (33%) which was associated with a rapid increase in fluorescence, reflecting an increase in exocytosis (Figure 6). In separate studies, exposure to shear (0.64 dyne/cm^2) also resulted in an increase in exocytosis (Figure 6). These findings suggest a functional link between exocytosis and ATP release in both MLC and MSC. There was no significant difference noted in the rate or magnitude of exocytosis between MLC and MSC in response to either of these mechanical stimuli.

ATP degradation

The concentration of extracellular ATP in bile is regulated not only through the rate of ATP release, but also through degradation pathways (23). To determine if differences exist in the kinetics of ATP degradation between MSC and MLC, the media bathing confluent cells was loaded with exogenous ATP (10 nM). Changes in bioluminescence were monitored continuously until relative ALU returned to basal levels. As shown in Figure 7, addition of ATP (10 nM) to MLC increased relative bioluminescence 2.7-fold. The time course of degradation was described by a single exponential ($y=ae^{-0.038\ min}$, r = 0.99). By comparison, addition of ATP to MSC increased bioluminescence 2.5-fold with a similar rate of degradation described by a single exponential ($y=ae^{-0034\ min}$, r = 0.99). Thus, MLC and MSC display functionally similar ATP degradation pathways.

Discussion

The present studies extend the observations regarding the specialized function of cholangiocytes by identifying and characterizing the elements of the purinergic signaling axis in cholangiocytes derived from distinct functional areas along the intrahepatic bile ducts. Utilizing molecular, pharmacological, and functional biophysical approaches the principal findings in these studies of mouse cholangiocytes are: i) both small and large cholangiocytes express a repertoire of both P2X and P2Y receptors; ii) both small and large cholangiocytes develop polarized epithelial monolayers with a high transepithelial resistance and demonstrate rapid increases in $[Ca^{2+}]_i$ and transepithelial secretion (I_{sc}) upon exposure to extracellular nucleotides; iii) nucleotide-stimulated secretion is dependent on IP3 receptor-mediated increases in $[Ca^{2+}]_i$ and Ca^{2+}-activated Cl^- channel activation; iv) both small and large cholangiocytes demonstrate mechanosensitive ATP release which is dependent on intact vesicular trafficking pathways; and v) the magnitude of mechanosensitive ATP release is significantly greater in small versus large cholangiocytes. Thus, these studies demonstrate that both small and large cholangiocytes express all components of the purinergic signaling axis and collectively, provide a working model for mechanosensitive ATP-stimulated secretion along intrahepatic bile ducts. Additionally, the ATP-mediated secretory pathway identified in the mouse small cholangiocytes, which do not exhibit secretin-stimulated secretion (3,17), represent the first identification of a secretory pathway in these specialized cells. The existence of a gradient along the biliary axis, wherein ATP released from small cholangiocytes “upstream” may represent an important paracrine signal to the “downstream” P2 receptor-expressing large cholangiocytes, has important implications for bile formation (Figure 8).

While regulated ATP release has been identified in all liver cells studied, including both human and rat hepatic parenchymal cells and biliary epithelial cells (20,22), these are the first studies to characterize ATP release in mouse cholangiocytes, and several observations deserve highlighting. First, the magnitude of ATP release from small cholangiocytes was significantly greater than that from large cholangiocytes. As the mechanism of cholangiocyte ATP release has not been identified, the cellular basis for this difference in ATP release cannot be determined. While CFTR has been proposed as a regulator of ATP release (12,24,25), MSC do not express CFTR (17), suggesting alternate ATP release pathways in these cells. One proposed alternate mechanism involves exocytosis of ATP-enriched vesicles. In fact, biliary cells possess a dense population of vesicles ~140 nm in diameter in the subapical space (26), and increases in cell volume increase the rate of exocytosis to values sufficient to replace ~30% of plasma membrane surface area within minutes. In the current studies, stimuli associated with ATP release were also associated with parallel increases in the rate of exocytosis, and disruption of vesicular trafficking significantly decreased ATP release. Notably, overall rates of exocytosis in response to mechanosensitive stimuli did not vary significantly between MLC and MSC, despite a significantly greater release of ATP from MSC, given the same stimulus. This may suggest the existence of distinct vesicle populations contributing to regulated ATP release. In fact, recent findings in rat liver cells suggest that a distinct population of ATP-enriched vesicles may contribute to regulated ATP release (27). In some cell types, the concentration of ATP within secretory vesicles may approach 50 mM (28) and, therefore, only several vesicles per cell may account for substantial differences in the concentration of ATP released into the extracellular space. Differences observed in the magnitude of ATP release between MSC and MLC may be related to variation in the regulation and/or trafficking of specific vesicles involved in ATP transport (either ATP-containing vesicles and/or vesicles transporting an ATP transporter to the membrane). This regulation may occur at the level of vesicle “priming”, trafficking, or membrane fusion/release, though clearly further work is required. Nonetheless, if these observations apply to *in vivo* conditions, greater ATP release from

small cholangiocytes would translate into a significant increase in the concentration of ATP in bile in the "upstream" intrahepatic ducts, given their smaller cross-sectional area and relative volume (29).

Second, it is notable that extracellular nucleotides elicit secretory responses when applied at both apical and basolateral membranes. The apical membrane specifically represents an anatomic orientation that is well suited for *hepatocyte-to-cholangiocyte* or *cholangiocyte-to-cholangiocyte* signaling by release of ATP into bile. This is notably distinct from secretin and other hormones that are delivered to the *basolateral* membrane through the bloodstream (1). ATP release from the hepatocyte canalicular membrane may signal to downstream small and large cholangiocytes through apical P2 receptor stimulation in a process known as hepatobiliary coupling. Hepatobiliary coupling has also been described for bile acids, which are released from the hepatocyte canalicular membrane and may be transported into "downstream" cholangiocytes via the apical Na^+-dependent bile acid transporter located on large, but not small, cholangiocytes (30). Interestingly, Ursodeoxycholic acid is associated with cholangiocyte ATP release and Cl^- secretion (24). Thus, the ductal concentration of ATP appears to be an important determinant of bile formation and may represent a final common pathway in coupling hepatocyte transport to cholangiocyte secretion.

Lastly, the relative importance of secretin- versus P2 receptor-mediated secretion, in bile formation is unknown. The molecular identity of the Cl^- channel(s) activated in response to ATP remains undefined in biliary epithelium, though it appears to be unrelated to CFTR (10). Furthermore, while we have previously identified the Ca^{2+}-activated K^+ channels, SK2 and IK-1, in rat and human biliary epithelial cells (7,8), the expression and contribution of these channels to secretion in mouse cholangiocytes has not been defined.

In conclusion, the present studies represent a functional characterization of the purinergic signaling axis in mouse cholangiocytes from distinct areas of the intrahepatic biliary tree. The findings support a model wherein ATP released from small cholangiocytes lining the "upstream" small intrahepatic bile ducts may contribute importantly to local purinergic signaling, serve as a source for ATP in bile, and represent an important paracrine signal to the large cholangiocytes lining the larger "downstream" bile ducts. Targeting P2 receptor-mediated signaling pathways in intrahepatic biliary epithelial cells may provide new and innovative strategies for stimulating bile formation in the treatment of cholestatic liver diseases.

Supplementary Material

Refer to Web version on PubMed Central for supplementary material.

Acknowledgments

Grant Support: This study was supported by the Cystic Fibrosis Foundation (FERANC08G0), the Children's Medical Center Foundation, and the National Institute of Diabetes, Digestive and Kidney Diseases (NIDDK) of the National Institute of Health DK078587 (APF) and DK054811 (GA) and VA Merit Award (GA).

Abbreviations

MLC	mouse large cholangiocytes
MSC	mouse small cholangiocytes
CFTR	cystic fibrosis transmembrane conductance regulator
Bz-ATP	2', 3'-O-(4-benzoyl-benzoyl)-ATP

Isc	short-circuit current
IP3	inositol 1,4,5-triphosphate

Reference List

1. Fitz, JG. Cellular mechanisms of bile secretion. In: Zakim, D.; Boyer, TD., editors. Hepatology. 3 ed.. Philadelphia: W.B. Saunders Company; 1996. p. 362-376.
2. Alpini G, Roberts S, Kuntz SM, Ueno Y, Gubba S, Podila PV, et al. Morphological, molecular, and functional heterogeneity of cholangiocytes from normal rat liver. Gastroenterology. 1996 May; 110(5):1636–1643. [PubMed: 8613073]
3. Francis H, Glaser S, Demorrow S, Gaudio E, Ueno Y, Venter J, et al. Small mouse cholangiocytes proliferate in response to H1 histamine receptor stimulation by activation of the IP3/CaMK I/CREB pathway. Am J Physiol Cell Physiol. 2008 Aug; 295(2):C499–C513. [PubMed: 18508907]
4. Ueno Y, Alpini G, Yahagi K, Kanno N, Moritoki Y, Fukushima K, et al. Evaluation of differential gene expression by microarray analysis in small and large cholangiocytes isolated from normal mice. Liver Int. 2003 Dec; 23(6):449–459. [PubMed: 14986819]
5. Martinez-Anso E, Castillo JE, Diez J, Medina JF, Prieto J. Immunohistochemical detection of chloride/bicarbonate anion exchangers in human liver. Hepatology. 1994; 19:1400–1406. [PubMed: 8188169]
6. Chari RS, Schutz SM, Haebig JA, Shimokura GH, Cotton PB, Fitz JG, et al. Adenosine nucleotides in bile. Am J Physiol. 1996; 270:G246–G252. [PubMed: 8779965]
7. Feranchak AP, Doctor RB, Troetsch M, Brookman K, Johnson SM, Fitz JG. Calcium-dependent regulation of secretion in biliary epithelial cells: the role of apamin-sensitive SK channels. Gastroenterology. 2004 Sep; 127(3):903–913. [PubMed: 15362045]
8. Dutta AK, Khimji AK, Sathe M, Kresge C, Parameswara V, Esser V, et al. Identification and functional characterization of the intermediate conductance Ca2+-activated K+ channel (IK-1) in biliary epithelium. Am J Physiol Gastrointest Liver Physiol. 2009 Sep 17.
9. McGill J, Basavappa S, Shimokura GH, Middleton JP, Fitz JG. Adenosine triphosphate activates ion permeabilities in biliary epithelial cells. Gastroenterology. 1994; 107:236–243. [PubMed: 8020667]
10. Dutta AK, Woo K, Doctor RB, Fitz JG, Feranchak AP. Extracellular nucleotides stimulate Cl- currents in biliary epithelia through receptor-mediated IP3 and Ca2+ release. Am J Physiol Gastrointest Liver Physiol. 2008; 295:G1004–G1015. [PubMed: 18787062]
11. Schlenker T, Romac JMJ, Sharara A, Roman RM, Kim S, LaRusso N, et al. Regulation of biliary secretion through apical purinergic receptors in cultured rat cholangiocytes. Am J Physiol. 1997; 273:G1108–G1117. [PubMed: 9374709]
12. Minagawa N, Nagata J, Shibao K, Masyuk AI, Gomes DA, Rodrigues MA, et al. Cyclic AMP regulates bicarbonate secretion in cholangiocytes through release of ATP into bile. Gastroenterology. 2007 Nov; 133(5):1592–1602. [PubMed: 17916355]
13. Woo K, Dutta AK, Patel V, Kresge C, Feranchak AP. Fluid flow induces mechanosensitive ATP release, calcium signalling and Cl- transport in biliary epithelial cells through a PKCzeta-dependent pathway. J Physiol. 2008 Jun 1; 586(Pt 11):2779–2798. [PubMed: 18388137]
14. Dranoff JA, Masyuk AI, Kruglov EA, LaRusso NF, Nathanson MH. Polarized expression and function of P2Y ATP receptors in rat bile duct epithelia. Am J Physiol Gastrointest Liver Physiol. 2001 Oct; 281(4):G1059–G1067. [PubMed: 11557527]
15. Doctor RB, Matzakos T, McWilliams R, Johnson S, Feranchak AP, Fitz JG. Purinergic regulation of cholangiocyte secretion: identification of a novel role for P2X receptors. Am J Physiol Gastrointest Liver Physiol. 2005 Apr; 288(4):G779–G786. [PubMed: 15528255]
16. Ishii M, Vroman B, LaRusso N. Isolation and morphologic characterization of bile duct epithelial cells from normal rat liver. Gastroenterology. 1989; 97:1236–1247. [PubMed: 2792660]
17. Glaser SS, Gaudio E, Rao A, Pierce LM, Onori P, Franchitto A, et al. Morphological and functional heterogeneity of the mouse intrahepatic biliary epithelium. Lab Invest. 2009 Apr; 89(4): 456–469. [PubMed: 19204666]

18. Gatof D, Kilic G, Fitz JG. Vesicular exocytosis contributes to volume-sensitive ATP release in biliary cells. Am J Physiol Gastrointest Liver Physiol. 2004 Apr; 286(4):G538–G546. [PubMed: 14604861]
19. Taylor AL, Kudlow BA, Marrs KL, Gruenert D, Guggino WB, Schwiebert EM. Bioluminescence detection of ATP release mechanisms in epithelia. Am J Physiol. 1998; 275:C1391–C1406. [PubMed: 9814989]
20. Feranchak AP, Fitz JG, Roman RM. Volume-sensitive purinergic signaling in human hepatocytes. J Hepatol. 2000 Aug; 33(2):174–182. [PubMed: 10952234]
21. Salter KD, Fitz JG, Roman RM. Domain-specific purinergic signaling in polarized rat cholangiocytes. Am J Physiol Gastrointest Liver Physiol. 2000 Mar; 278(3):G492–G500. [PubMed: 10712270]
22. Feranchak AP, Roman RM, Doctor RB, Salter KD, Toker A, Fitz JG. The lipid products of phosphoinositide 3-kinase contribute to regulation of cholangiocyte ATP and chloride transport. J Biol Chem. 1999; 274:30979–30986. [PubMed: 10521494]
23. Dubyak GR, El-Moatassim C. Signal transduction via P2-purinergic receptors for extracellular ATP and other nucleotides. Am J Physiol. 1993; 265:C577–C606. [PubMed: 8214015]
24. Fiorotto R, Spirli C, Fabris L, Cadamuro M, Okolicsanyi L, Strazzabosco M. Ursodeoxycholic acid stimulates cholangiocyte fluid secretion in mice via CFTR-dependent ATP secretion. Gastroenterology. 2007 Nov; 133(5):1603–1613. [PubMed: 17983806]
25. Braunstein GM, Roman RM, Clancy JP, Kudlow BA, Taylor AL, Shylonsky VG, et al. Cystic fibrosis transmembrane conductance regulator facilitates ATP release by stimulating a separate ATP release channel for autocrine control of cell volume regulation. J Biol Chem. 2001 Mar 2; 276(9):6621–6630. [PubMed: 11110786]
26. Doctor RB, Dahl R, Fouassier L, Kilic G, Fitz JG. Cholangiocytes exhibit dynamic, actin-dependent apical membrane turnover. Am J Physiol Cell Physiol. 2002 May; 282(5):C1042–C1052. [PubMed: 11940520]
27. Feranchak AP, Lewis MA, Kresge C, Sathe M, Bugde A, Luby-Phelps K, et al. Initiation of purinergic signaling by exocytosis of ATP-containing vesicles in liver epithelium. J Biol Chem. 2010 Mar 12; 285(11):8138–8147. [PubMed: 20071341]
28. Bergendorff A, Uvnas B. Storage properties of rat mast cell granules in vitro. Acta Physiol Scand. 1973 Feb; 87(2):213–222. [PubMed: 4718205]
29. Masyuk, TV.; Masyuk, AI.; Ritman, EL.; LaRusso, NF. Three-dimensional reconstruction of the rat intrahepatic biliary tree: physiologic implications. In: Alpini, G.; Alvaro, D.; Marzioni, M.; Lesage, G.; LaRusso, N., editors. The pathophysiology of biliary epithelia. Georgetown, TX: Landes Bioscience; 2004. p. 60-71.
30. Alpini G, Glaser SS, Rodgers R, Phinizy JL, Robertson WE, Lasater J, et al. Functional expression of the apical Na+-dependent bile acid transporter in large but not small rat cholangiocytes. Gastroenterology. 1997 Nov; 113(5):1734–1740. [PubMed: 9352879]

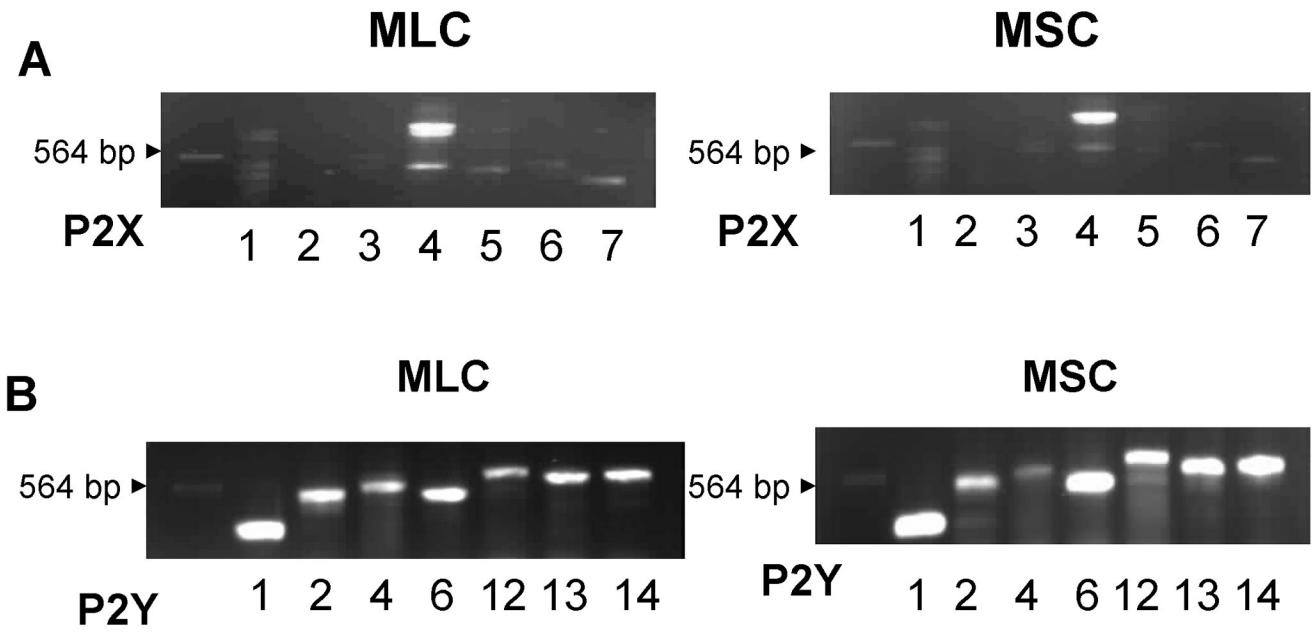

Figure 1.

Mouse cholangiocytes express P2 receptors. Molecular expression of P2X and P2Y receptor subtypes was evaluated by RT-PCR with specific oligonucleotides. A. P2X receptor expression. P2X4 is the predominant P2X receptor in both mouse large (MLC), left panel, and mouse small (MSC), right panel, cholangiocytes. B. P2Y receptor expression. Both MLC and MSC express multiple P2Y receptor subtypes, including P2Y1, P2Y2, P2Y4, P2Y6, P2Y12, P2Y13, and P2Y14. The arrow head indicates 564 base pair λDNA-Hind III fragment.

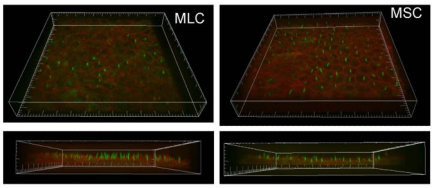

Figure 2.
MLC and MSC form polarized monolayers. MLC (left) and MSC (right) were cultured on cover glass for 5 days and stained for acetylated α-tubulin, as a cilia marker protein (green), and phalloidin, for actin localization (red). Bottom panels represent Z-axis to highlight cilia. Scale, small hatch marks=5 μm.

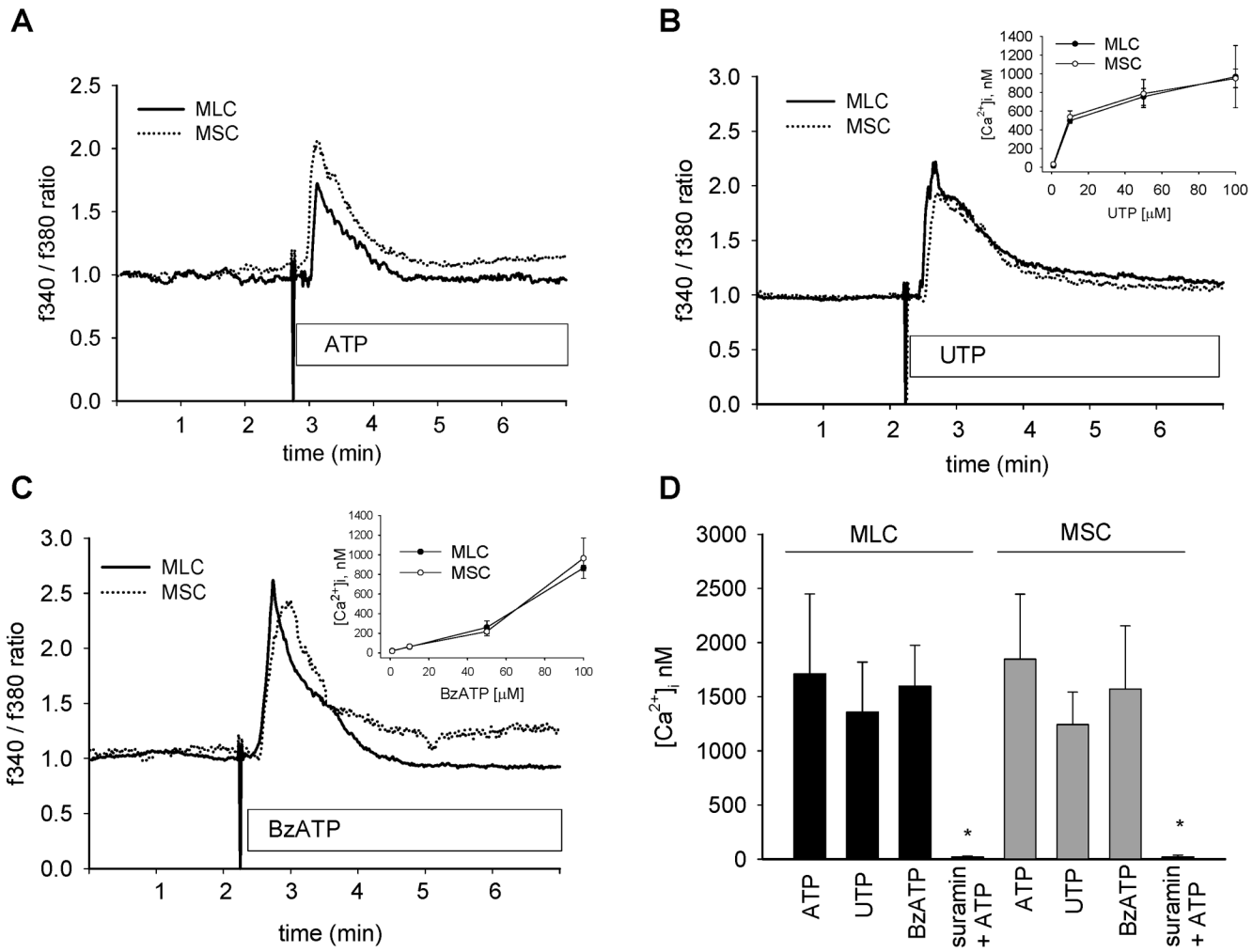

Figure 3.

P2 receptor agonists increase intracellular Ca^{2+} in mouse cholangiocytes. MLC and MSC cells were loaded with fura-2-AM and exposed to extracellular nucleotides, ATP (100 μM), UTP (100 μM), or Bz-ATP (100 μM) as indicated. The y axis values represent the ratio of fluorescence at 340 and at 380 nm. A, B, C. Representative studies. Ca^{2+}-fluorescence increased rapidly in both MLC (solid line) and MSC (dotted line) upon exposure to nucleotides. Insets, B and C, demonstrate dose-response for respective agonist. D. Cumulative data. Values represent the maximal $[Ca^{2+}]_i$ in nM. $[Ca^{2+}]_i$ was calculated based on maximal and minimal Ca^{2+} fluorescence obtained by exposure to ionomycin (5 μM) and EGTA (10 mM), respectively (N=3–6 each). *Suramin significantly inhibits ATP-stimulated $[Ca2+]_i$, $p<0.05$.

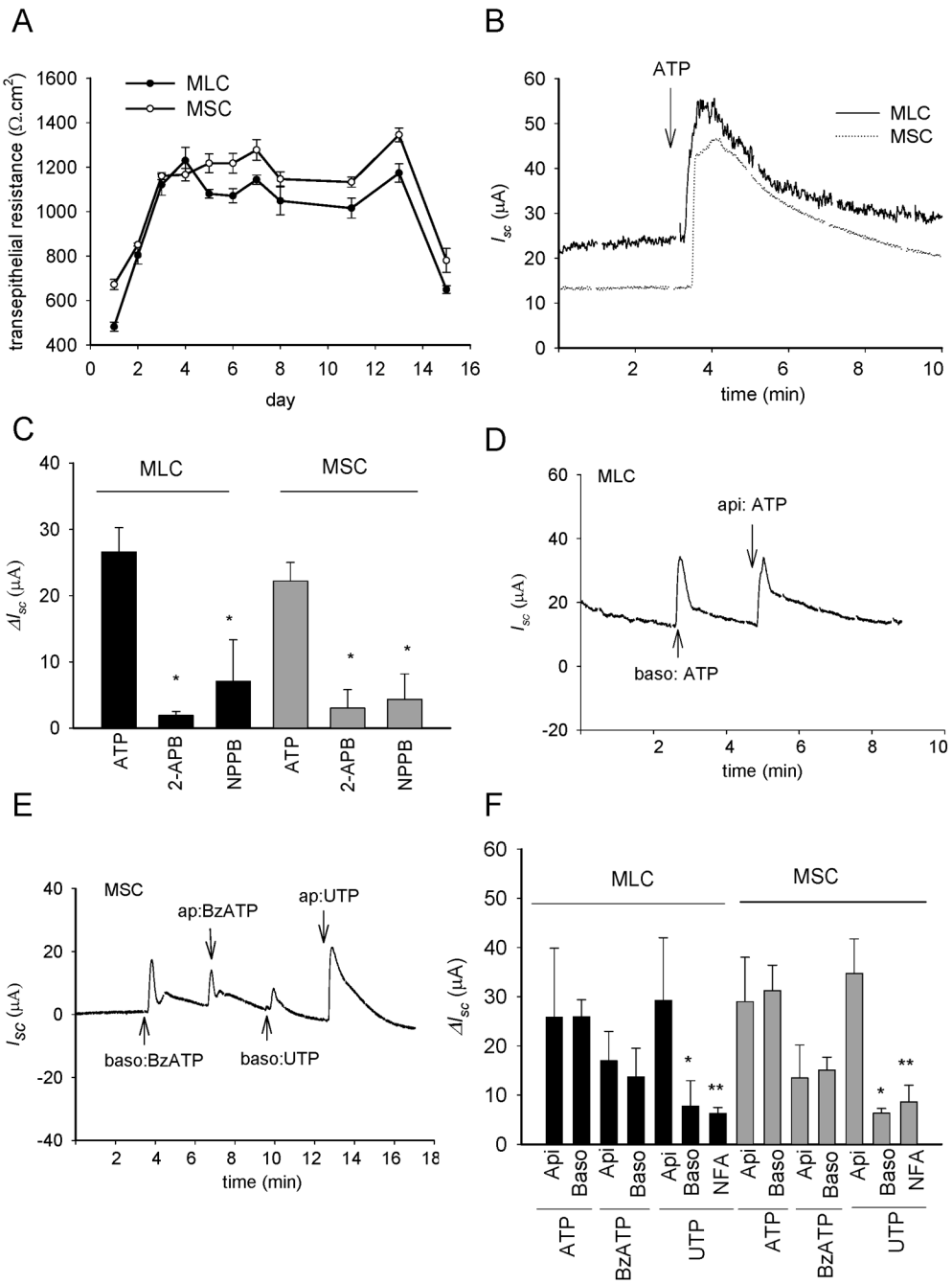

Figure 4.

Mouse cholangiocytes form polarized monolayers and exhibit increases in transepithelial Cl^- secretion in response to extracellular nucleotides. A. Transmembrane resistance ($\Omega.cm^2$) was measured at the time points indicated in MLC and MSC grown on semi-permeable filters. B. Representative tracings of MLC or MSC mounted in Ussing chamber. The y-axis represents short-circuit current (I_{sc}) across monolayers measured under voltage-clamp conditions (μA). ATP (100 μM), added to the apical chamber, significantly increased I_{sc}. C. Cumulative data demonstrating effect of 2-APB or NPPB on ATP-stimulated I_{sc}. The *y*-axis values are reported as ΔI_{sc} (maximum I_{sc} – basal I_{sc}). * 2-APB or NPPB significantly inhibit ATP-stimulated ΔI_{sc} ($p < 0.05$, n= 3–9 each). D. Representative recording of apical or

basolateral additions of ATP (100 μM)-stimulated I_{sc} in MLC. E. Representative recording of apical or basolateral additions of BzATP (100 μM) and UTP (100 μM) in MSC. F. Cumulative data. Values (mean ± SEM) represent Δ I_{sc}. Api = apical addition, and Baso = basolateral addition, of respective reagent (n=4–12 each). *Apical addition of UTP increases I_{sc} > than basolateral addition ($p<0.05$). ** Niflumic acid (NFA, 250 μM) inhibits UTP-stimulated Isc ($p<0.05$).

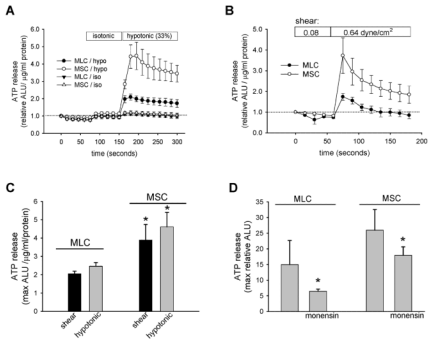

Figure 5.

Mechanosensitive ATP release from mouse cholangiocytes. ATP in the extracellular media was detected using the luciferin-luciferase assay and quantified as arbitrary light units (ALU). The y-axis represents relative increase from basal luminescence (expressed as relative ALU/µg/ml protein). A. Cell swelling-induced ATP release from confluent MLC and MSC. Addition of isotonic media to cells led to a small increase in luminescence. Dilution of media 33% by the addition of water (indicated by bar) led to an increase in ATP release in both MSC (open circles) and MLC (closed circles) much greater than control cells exposed to only a second isotonic exposure. B. Shear-stimulated ATP release from confluent MLC (closed circles) and MSC (open circles) cells. Cells were perfused with Optimem and 60 µl aliquots were taken from the efflux every 30 seconds, added to standard L-L reagent, and immediately placed in the Luminometer for luminescence measurement. Bars along top indicate length of low flow (shear 0.08 dyne/cm^2) and high flow (shear 0.64 dyne/cm^2) exposure. C. Cumulative data demonstrating relative ATP release from both MLC and MSC in response to shear (0.64 dyne/cm^2, black bar) and hypotonic exposure (33% dilution, grey bar). Values represent maximum ATP concentration within 30 seconds of shear or hypotonic exposure, mean ± SEM, *ATP release is significantly greater in MSC vs MLC, $p<0.05$. D. Inhibition of vesicular trafficking inhibits swelling-induced ATP release in MLC and MSC. *Monensin (100 µM X 30 minutes) significantly inhibits ATP release in response to hypotonic exposure (33% dilution); $p<0.05$, n=4–6 each.

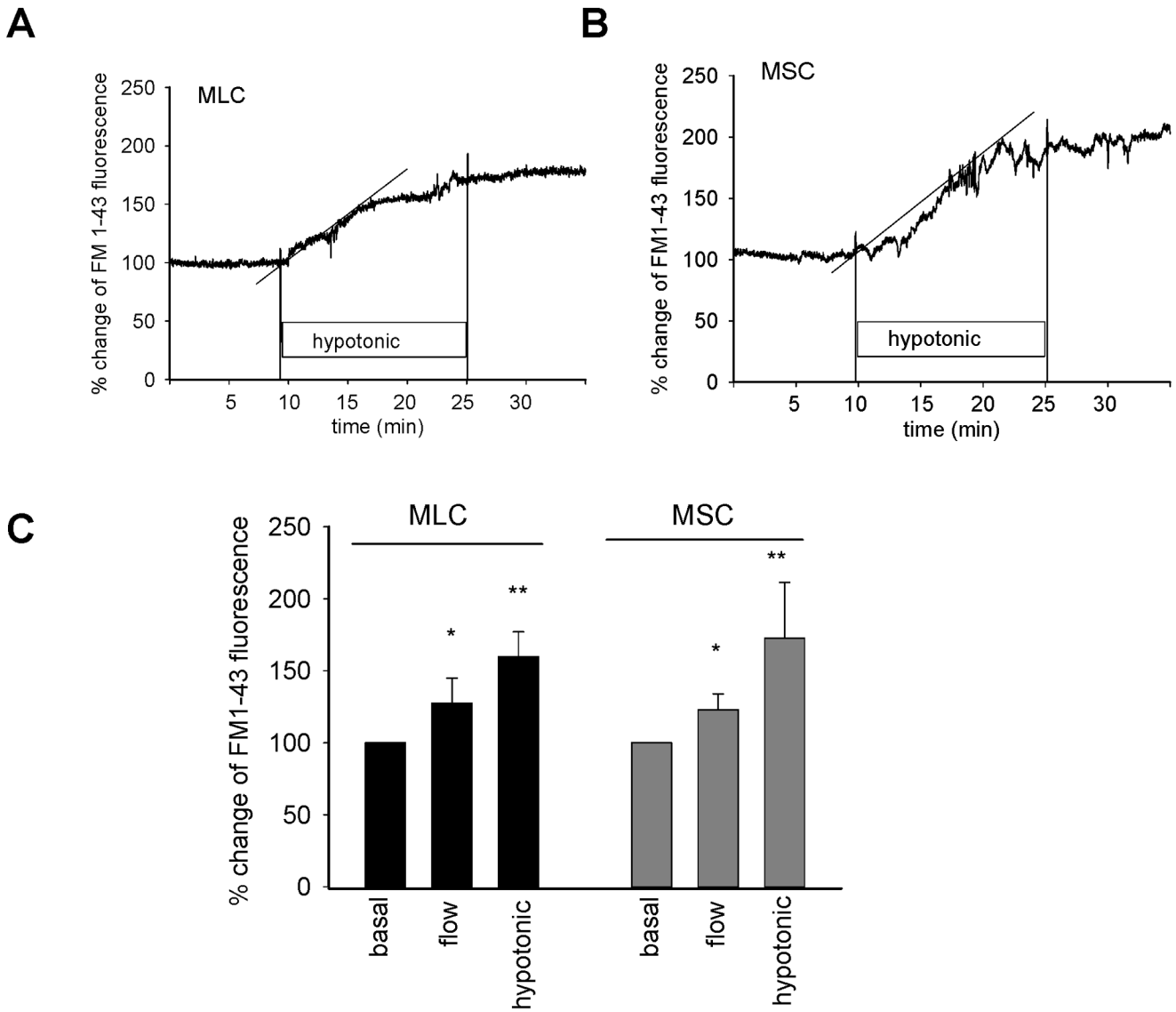

Figure 6.

Mechanosensitive exocytosis. MLC and MSC cells on coverglass were loaded with FM1-43 and exposed to shear or hypotonicity as indicated. The values of the y-axis represent % increase in membrane fluorescence. A & B. Representative figures of swelling-induced exocytosis. FM1-43 fluorescence was stabilized in isotonic buffer before the cells were exposed to hypotonic buffer (33%). Hypotonic exposure rapidly increased plasma membrane fluorescence as a result of vesicular exocytosis in both MLC (A) and MSC (B). Dotted line represents best-fit regression analysis. E. Cumulative data demonstrating maximum magnitude of exocytosis in both MLC and MSC in response to shear (0.64 dyne/cm^2) or hypotonic (33%) exposure. Values represent maximum % change in FM1-43 fluorescence (n=5–6 each). *p<0.05 shear versus basal; **p<0.05 hypotonic exposure versus isotonic.

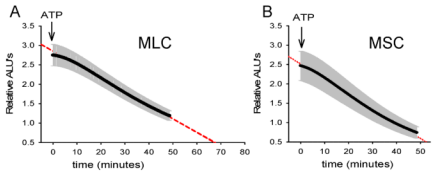

Figure 7.

Kinetics of ATP degradation in mouse cholangiocytes. ATP degradation was assessed after addition of ATP (10 nM, at arrow) to apical membrane of confluent MLC (panel A) and MSC (panel B). The y-axis represents relative arbitrary light units (ALU). Values represent means (black points) ± SEM (grey bars); n = 4 monolayers/time point. Dashed line represents best-fit regression.

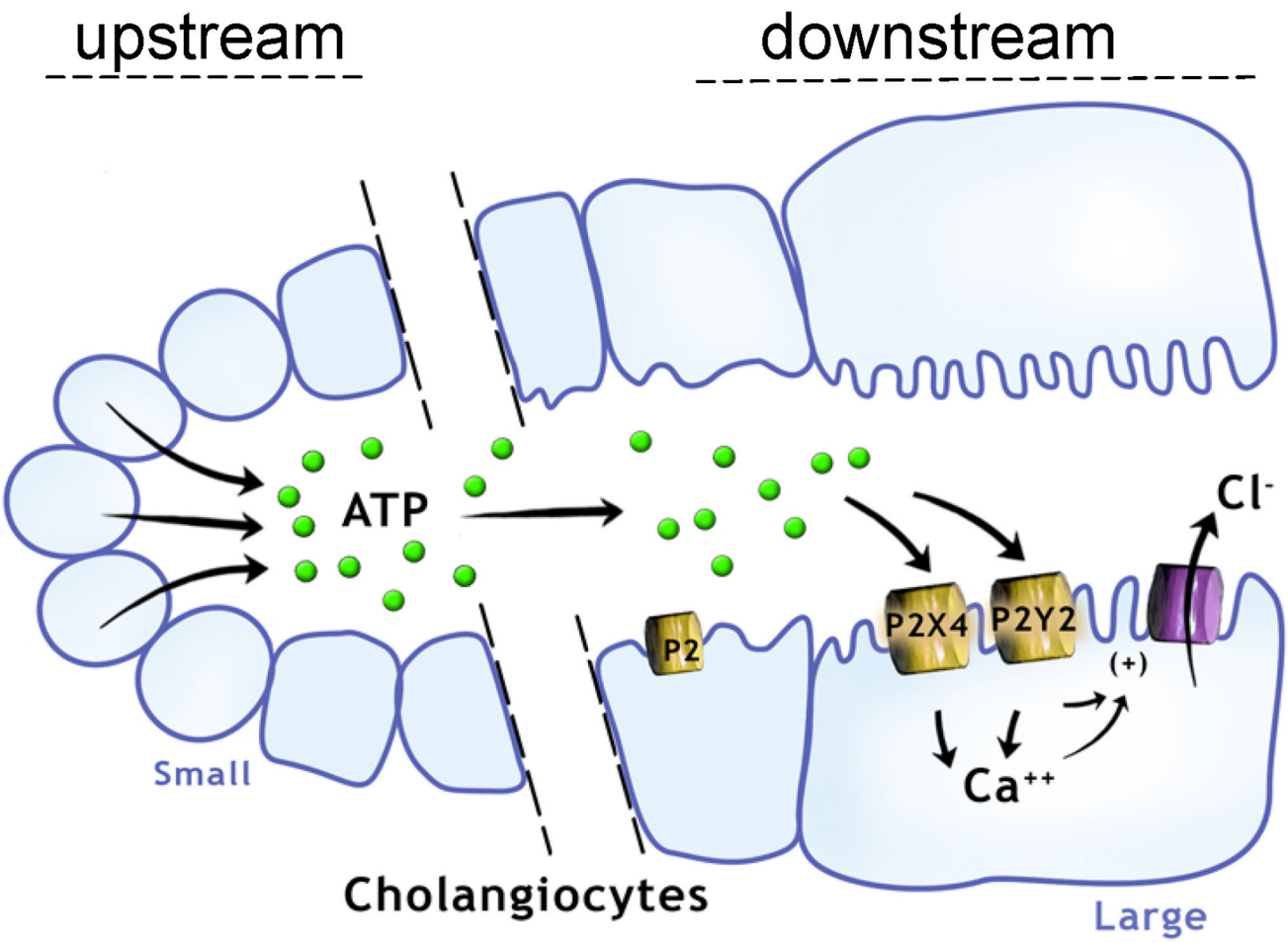

Figure 8.
Proposed model of the purinergic signaling axis along the intrahepatic bile duct. ATP released from small cholangiocytes lining the “upstream” small intrahepatic bile ducts may contribute importantly to local purinergic signaling, serve as a source for ATP in bile, and represent an important paracrine signal to the large cholangiocytes lining the larger “downstream” bile ducts. Both small and large cholangiocytes express a full array of P2 receptors and respond to extracellular nucleotides with increases in $[Ca^{2+}]_i$ and Cl^- secretion.